

Efficient Simulation and Abuse Modeling of Mechanical-Electrochemical-Thermal Phenomena in Lithium-Ion Batteries

Presenter: Shriram Santhanagopalan
National Renewable Energy Laboratory
June 20, 2018

Team: Chao Zhang, Chuanbo Yang, Qibo Li, Lei Cao,
Andrew Colclasure, **National Renewable Energy Laboratory**
Joshua Lamb, **Sandia National Laboratories**
Daniel Abraham, Pierre Yao, Dennis Dees, **Argonne National Laboratory**
Kelly Carney, **Forming Simulation Technologies LLC**
Amos Gilat, **Ohio State University**

DOE Vehicle Technologies Office
2018 Annual Merit Review and Peer Evaluation Meeting

Overview

This project was awarded in response to VTO FY15 Lab Call.

Timeline

- Project start date: Oct. 2015
- Project end date: Sept. 2018
- Percent complete: 75%

Budget

- Total project funding: \$ 3.15M
 - DOE share: 100%
- Funding received in FY 2016: \$1.05M
- Funding received in FY 2017: \$1.05M
- Funding received in FY 2018: \$ 600k

Barriers

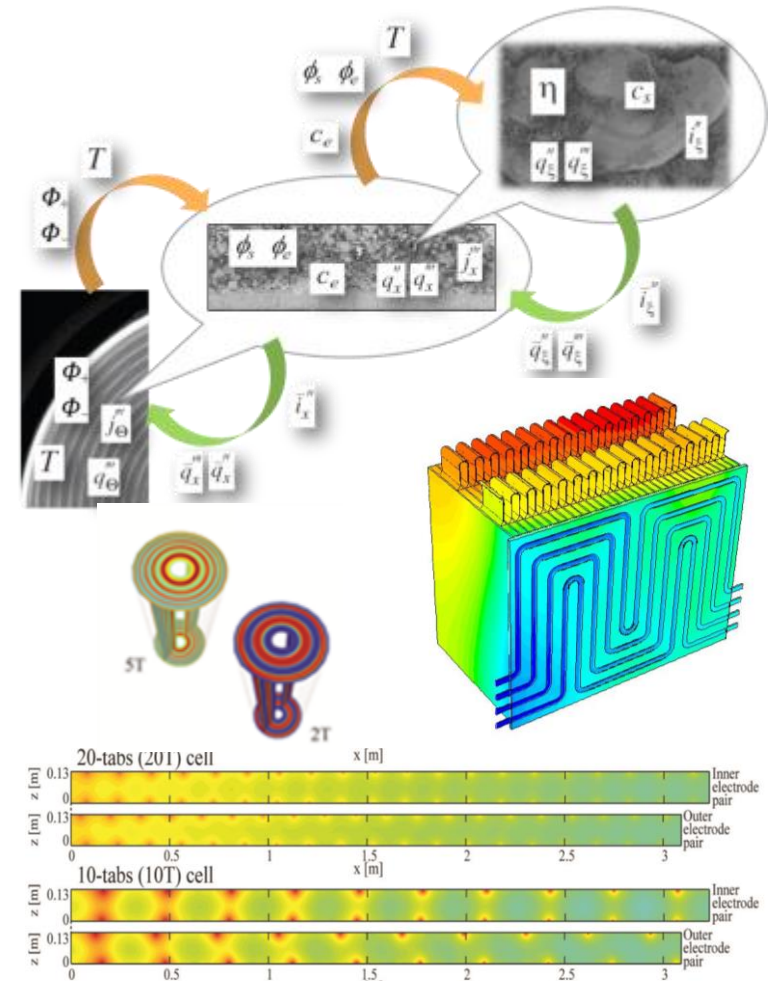
- Gap between modeling tools and cell design process in the industry
- Lack of simulation tools integrating mechanical failure and abuse response of batteries for practical assessment of battery safety
- Limited understanding of complex failure mechanisms resulting in expensive over-design of batteries

Partners

- Argonne National Laboratory (ANL)
 - Pouch cells and data for parameter estimation
- Sandia National Laboratories (SNL)
 - Cell-level mechanical abuse testing for validation of mechanical models
- Forming Simulation Technologies (FST), Ohio State University (OSU), George Mason University (GMU)
 - Integration with ANSYS and LS-DYNA
- Lead: National Renewable Energy Laboratory (NREL)

Relevance

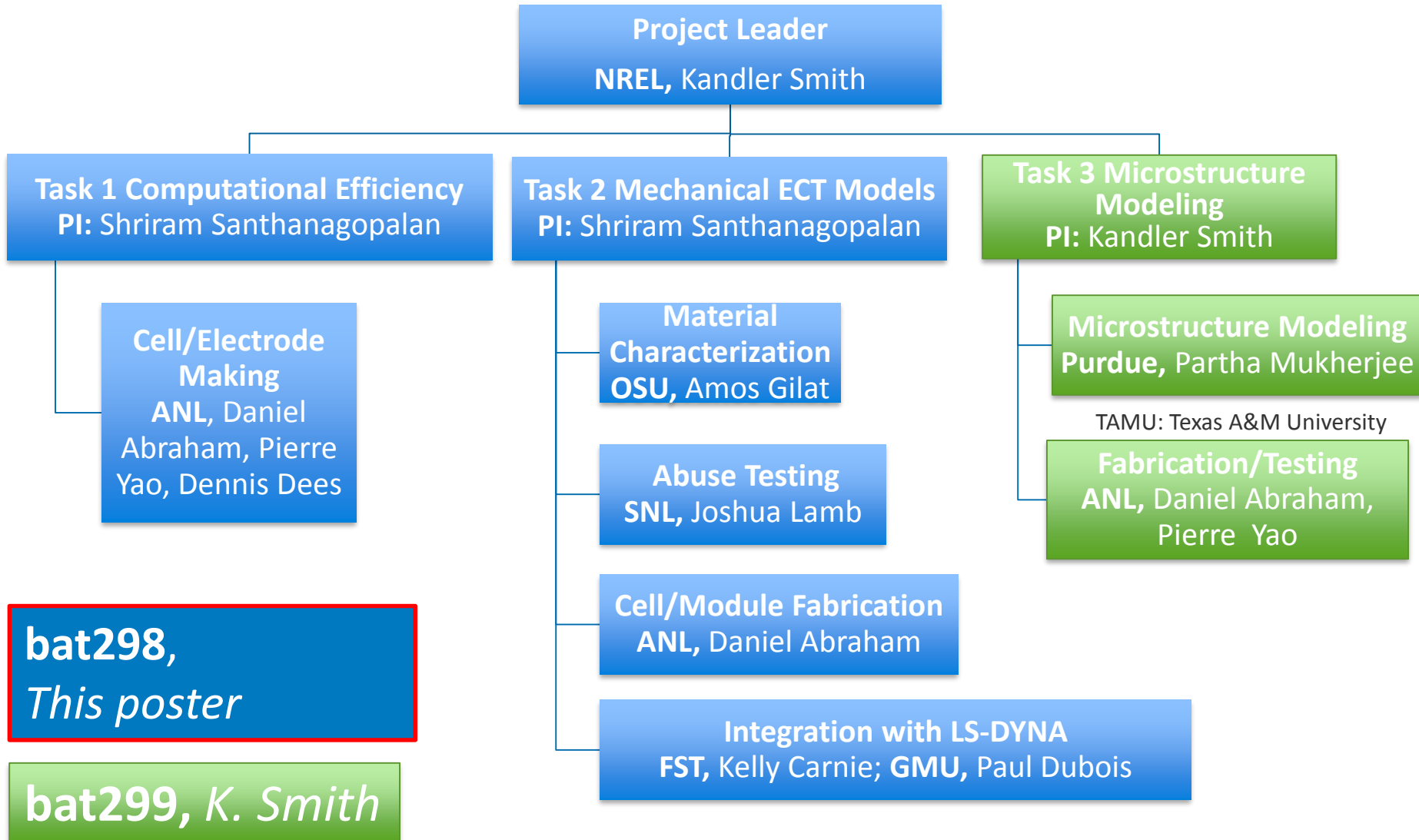
- VTO launched the Computer-Aided Engineering of Batteries (CAEBAT) project to develop validated modeling tools to accelerate development of batteries, in support of vehicle electrification R&D to reduce dependence on imported oil.
- Over 40 different end users from the community have adapted the Multi-Scale Multi-Domain (MSMD) modeling approach developed under CAEBAT.
- Feedback from the first few sets of end-users has helped us identify priorities that will enable wider use of model-based design:
 - Standardize identification of the model parameters
 - Increase computational efficiency
 - Extend the models to include mechanical failure of cells and packaging components
 - Close gaps between materials R&D and CAEBAT modeling tools
- We are now licensing out beta versions of NREL models to the industry and academic partners to identify technical gaps in simulation capabilities.



MSMD models previously developed in CAEBAT have been widely adapted in the community and helped us identify gaps.

Project Structure

Project Title: Computer-Aided Battery Engineering Consortium



Relevance

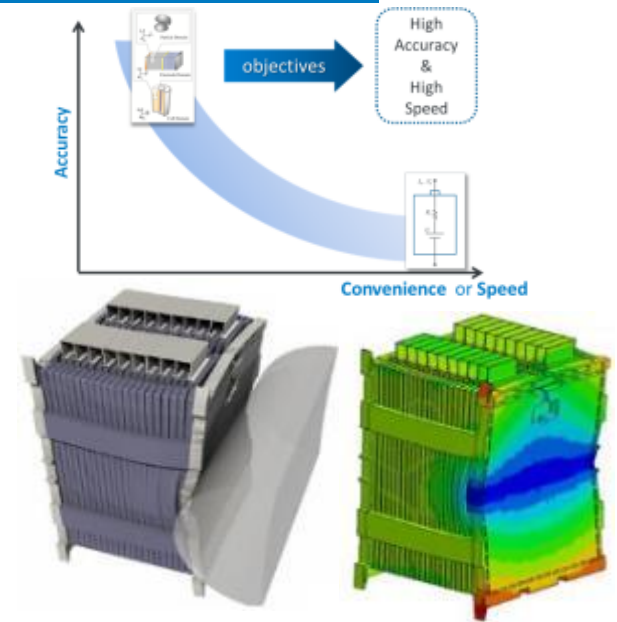
Objectives for March 2017 – March 2018

Computational Efficiency

- Calibrate parameters in a Newman-type model for ANL CAMP electrodes of varying thickness and porosity

Mechanical-Electrochemical-Thermal (MECT) Models

- Demonstrate *implementation* of a computationally efficient approach to implement simultaneous coupling of mechanical response at the cell level, to electrochemical-thermal (ECT) models
- Develop mechanical models to assess impact of aging of lithium-ion cells on safety
- Present comparison of multi-cell propagation models against test data from SNL



Initial demonstration of efficient thermal, electrochemical, and mechanical models

Impact: By making disruptive CAE design tools available on desktop computers for use by the battery community, this effort supports the following goals identified by the VTO:

1. Reduce the number and duration of battery test cycles in the industry to enable a path to \$80/kWh electric vehicle (EV) battery costs by drastically
2. Reduce module/pack costs by maximizing insight gathered on failure modes in batteries from a limited subset of tests currently performed

Milestones

	Milestone Name/Description	Deadline	Milestone Type	Status
Computational Efficiency	M 1.1 MSMD identification and simulation of graphite/NCM532 system	01/31/2017	Qtr. Prog. Meas.	Done
	M 1.2 Submit journal article on analysis of NCM532 solid state diffusivity concentration dependence from GITT experiments	11/30/2017	Qtr. Prog. Meas.	Done
	M 1.3 Prepare presentation for DOE Annual Merit Review	04/30/2017	Qtr. Prog. Meas.	Done
	M 1.4 Report summarizing ability of macro-homogeneous model to predict performance of ANL CAMP electrodes of varying thickness and porosity	03/31/2018	Qtr. Prog. Meas.	Done
Mechanical Abuse	M 2.1 Demonstrate simultaneous coupling in MECT model that shows interaction of mechanical deformation with the thermal response of the cell under different strain rates within 10% error against data	03/31/2016	Annual SMART (Go/No-Go)	Go
	M 2.2 Draft documentation describing the mechanical tests procedure for development and validation of constitutive models for individual battery components	07/31/2017	Annual SMART (Go/No-Go)	Go ⁺
	M 2.3 Interim update on mechanical models demonstrating damage propagation	12/31/2017	Qtr. Prog. Meas.	Done
	M 2.4 Report summarizing model valuation for MECT simulations	04/30/2018	Qtr. Prog. Meas.	Delayed

⁺ Based on findings from this milestone, additional measurements were performed to characterize mechanical properties of electrodes at higher strain rates and under failure due to shear on top of the scheduled test plan for this milestone.

Task 1 – Computational Efficiency

Approach



Experimental setup to cycle cells for collecting data
Photo Credit: Lei Cao, NREL

Pre-processing and filtering of raw data



Format data from native formats for battery cyclers

Setup baseline MSMD Inputs

$$\frac{\partial}{\partial x} \left(\frac{D_s}{L} \frac{\partial c_s}{\partial x} \right) + \frac{\partial}{\partial x} \left(\kappa_d^{eff} \frac{\partial \ln c_s}{\partial x} \right) + j_x^{irr} = 0$$

$$\kappa_d^{eff} = \kappa_d \varepsilon_p^p$$

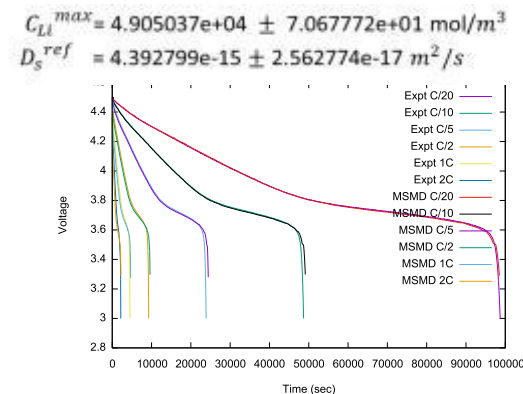
$$\kappa_d^{eff} = \frac{2RT\kappa_d^{eff}}{F} (t_+^0 - 1) \left(1 + \frac{d \ln f_+}{d \ln c_s} \right)$$

$$\frac{\partial(\varepsilon_s c_s)}{\partial t} = \frac{\partial}{\partial x} \left(D_s^{eff} \frac{dc_s}{dx} \right) + \frac{1 - t_+^0}{F} j_x^{irr} - \frac{i_s^*}{F} \frac{\partial t_+^0}{\partial x}$$

MSMD-Model

Fitting of model to data

- Python script parses data to meet model needs
- Parameter estimation based on Levenberg-Marquardt algorithm
- Workflow independent of model(s)/data set(s)
- Can use the same approach for multiple models and/or datasets – as long as the list of inputs and outputs are standardized (e.g., using the OAS)
- Process can be easily wrapped with a GUI as workflow stabilizes



Calibrated Model and Parameters

Leveraging Electrode Library from ANL-CAMP

- 14 graphite & NMC532 electrodes of varying thickness and porosity were manufactured and electrochemically characterized by ANL

	Calendering	Name	Coating thickness [μm]	Volume fraction			Density [mg.cm ⁻²]		Loading [mAh.cm ⁻²]	Experimental C-rate ^c [mAh.g _{active} ⁻¹]
				Pore	Active material	CBD	Coating	Active material	Active material	
NMC532	No	1-UNCAL	160	49.1	39.7	11.2	33.09	29.78	8.27	179
	Yes	1-CAL	129	36.8	49.3	13.9				178
	No	2-UNCAL	140	51.8	37.6	10.6	27.39	24.65	6.84	179
	Yes	2-CAL	108	37.5	48.8	13.7				180
	No	3-UNCAL	106	47.4	41.0	11.6	22.60	20.40	5.66	183
	Yes	3-CAL	88	36.6	49.5	13.9				182
	Yes	4-CAL	34	33.5	51.9	14.6	9.17	8.25	2.29	178
Graphite	No	5-UNCAL	205	50.7	44.6	4.7	21.89	20.1	7.48	336
	Yes	5-CAL	165	38.8	55.4	5.8				300
	No	6-UNCAL	173	51.8	43.6	4.6	18.08	16.6	6.17	330
	Yes	6-CAL	131	36.3	57.7	6.0				282
	No	7-UNCAL	140	51.4	44.0	4.6	14.70	13.5	5.02	351
	Yes	7-CAL	110	38.0	56.1	5.9				351
	Yes	8-CAL	44	38.4	55.8	5.8	5.88	5.51	2.05	363

CAL: calendared, CBD: carbon/binder domain, UNCAL: uncalendared

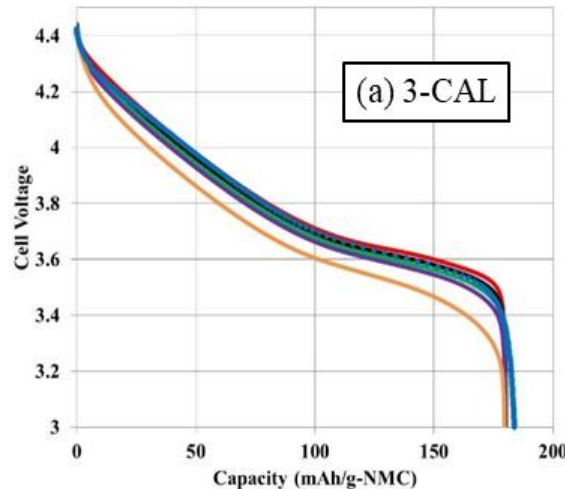
Model Comparison with NMC532 Discharge Data

88 μm (3-CAL)

Small electrolyte concentration gradients

Capacity is not sensitive to Bruggeman exponent

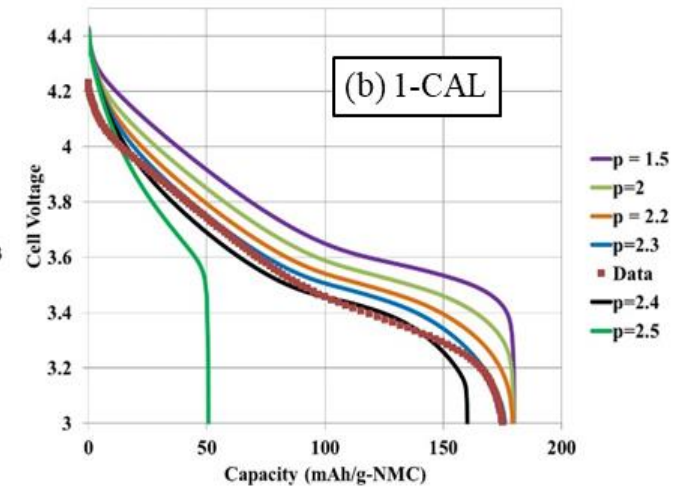
1C discharge data vs model with varying Bruggeman exponent, p



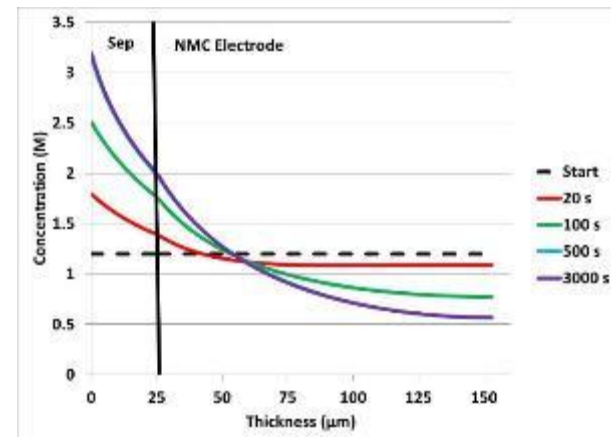
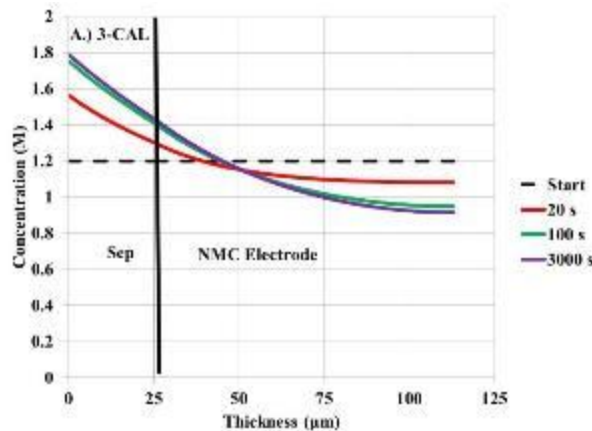
129 μm (1-CAL)

Large electrolyte concentration gradients

Capacity is sensitive to Bruggeman exponent



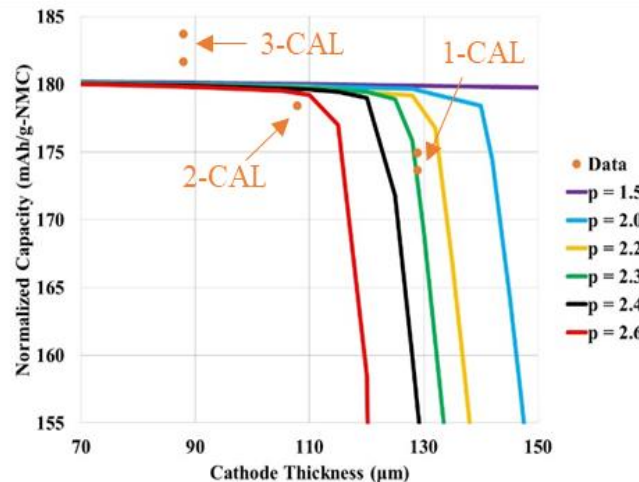
Electrolyte concentration profiles at 1C (best fit p)



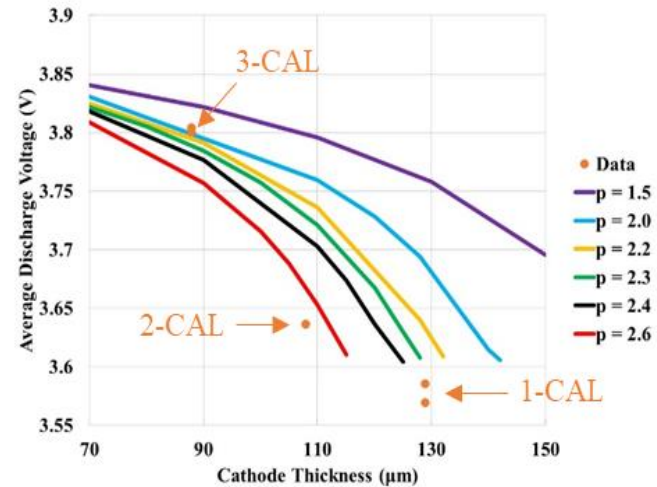
Model Compares Well. Fitted Tortuosity Used to Validate Microstructure Model*

Model run
with varying
Bruggeman
exponent

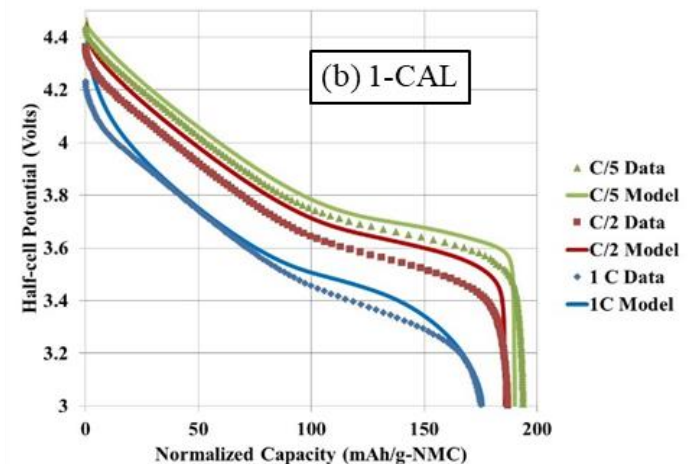
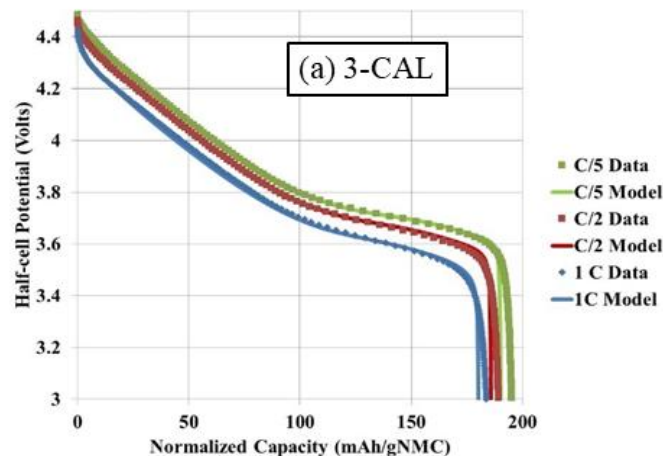
Normalized capacities



Average discharge voltage



Model
comparison at
varying C-rates
(best fit p)



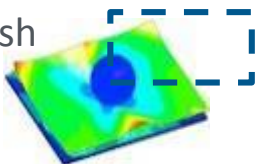
*See microstructure modeling poster bat299

Task 2 – Mechanical- Electrochemical-Thermal Modeling of Abuse Phenomena

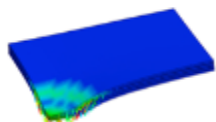
Mechanical Modeling Approach

Objective: Predict battery behavior during a crash event to optimize safety and weight reduction

Displacement under
Crush



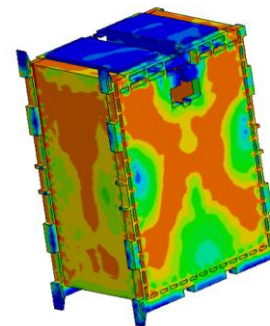
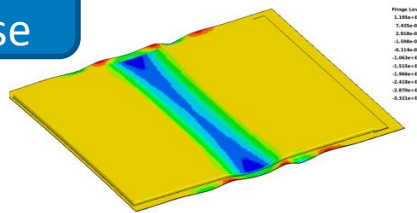
Step 2: Explicit simulations
parameterize material response



Current density
under short circuit

Predicts cell
temperatures to $\pm 10^\circ\text{C}$

Step 4: Scale to module level



Step 3: Simulate cell-level
response for multiple cases

Step 5: Validate against
experimental data

Goal: Identify localized failure modes
and onset loads to within 30 MPa



Step 1: Start with component and
cell-level test results as input

Sample Input:

- Stress-strain curves for cell components (separator, current collector, etc.)
- Failure strengths for particles
- Mechanical data for cell packaging
- Temperature vs. C-rate for cell
- Abuse reaction data from calorimetry for specific chemistries

Sample Output:

- Current distribution among the different cells within the module
- Localized heat generation rates far away from damage zone
- Stress distribution across multiple parts of the battery module

Photo Credits: Jim
Marcecki, Ford

Approach: Constitutive Model Development

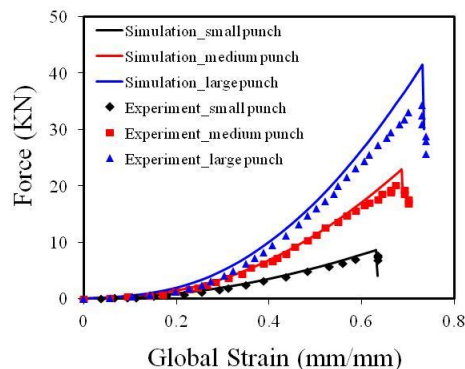
Step 1. Develop physics-based component models

$$\sigma_{ij,j} + \rho f_i = \rho u_{i,tt}$$

$$\sigma_{ij} = C_{ijkl} \gamma_{kl}$$

$$E = \begin{cases} E_{max} e^{\beta(\epsilon - \epsilon_p)} & \epsilon < \epsilon_p \\ E_{max} & \epsilon \geq \epsilon_p \end{cases}$$

Step 3. Validate against independent data set

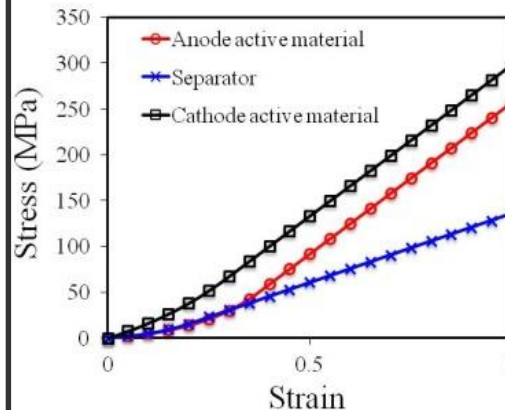


Cell-level data vs. model

Step 2. Obtain model parameters

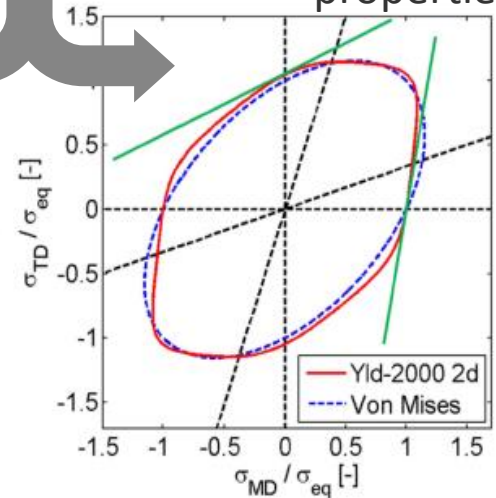
Approach a:

Calibrates parameters out of component-level stress-strain data



Approach b:

Phenomenological models for material properties



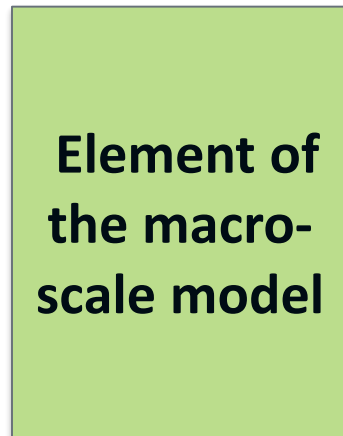
$$\bar{\sigma}(\sigma) = \bar{\sigma}(\sigma_{xx}, \sigma_{yy}, \sigma_{xy}) = \frac{1}{2^{1/a}} (|S'_I - S'_{II}|^a + |2 \cdot S''_I + S''_{II}|^a + |S'_I + 2 \cdot S''_{II}|^a)^{1/a}$$

Approach: Multiscale Simultaneously Coupled Modeling Framework

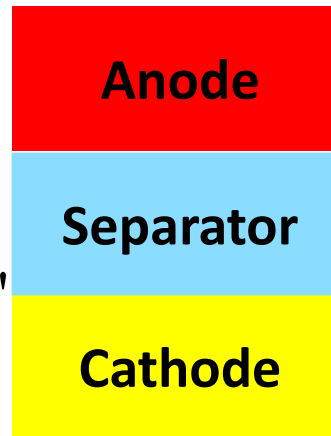
Macro-scale 3D homogenized
mechanical-thermal model

Meso-scale quasi-3D
mechanical-thermal model

Pseudo 2D
electrochemical-thermal model



$$\begin{array}{c} \xrightarrow{d\bar{e}, dt, t, T} \\ \xleftarrow{\bar{S}, S_i, \bar{e}, e_i, T'} \end{array}$$



$$\begin{array}{c} \xrightarrow{R_{short}, Ks_i, dt', t', T} \\ \xleftarrow{T'} \end{array}$$

$$\sigma_{ij} = C_{ijkl} \epsilon_{kl}$$

Approach for Coupling Methodology

- Retain fidelity of damage models at the component level (e.g., separate failure criteria for separator, current collector, etc.)
- Solve for potential and temperature as additional degrees of freedom at the component scale
- Simulate multi-cell effects using a micro-mechanical homogenization scheme

$$\begin{Bmatrix} \sigma_{11} \\ \sigma_{22} \\ \sigma_{12} \\ \sigma_{33} \\ \sigma_{23} \\ \sigma_{13} \end{Bmatrix} = \begin{bmatrix} C_{11} & C_{12} & C_{16} & C_{13} & C_{14} & C_{15} \\ C_{12} & C_{22} & C_{26} & C_{23} & C_{24} & C_{25} \\ C_{16} & C_{26} & C_{66} & C_{36} & C_{46} & C_{56} \\ C_{13} & C_{23} & C_{36} & C_{33} & C_{34} & C_{35} \\ C_{14} & C_{24} & C_{46} & C_{34} & C_{44} & C_{45} \\ C_{15} & C_{25} & C_{56} & C_{35} & C_{45} & C_{55} \end{bmatrix} \begin{Bmatrix} \epsilon_{11} \\ \epsilon_{22} \\ \epsilon_{12} \\ \epsilon_{33} \\ \epsilon_{23} \\ \epsilon_{13} \end{Bmatrix}$$

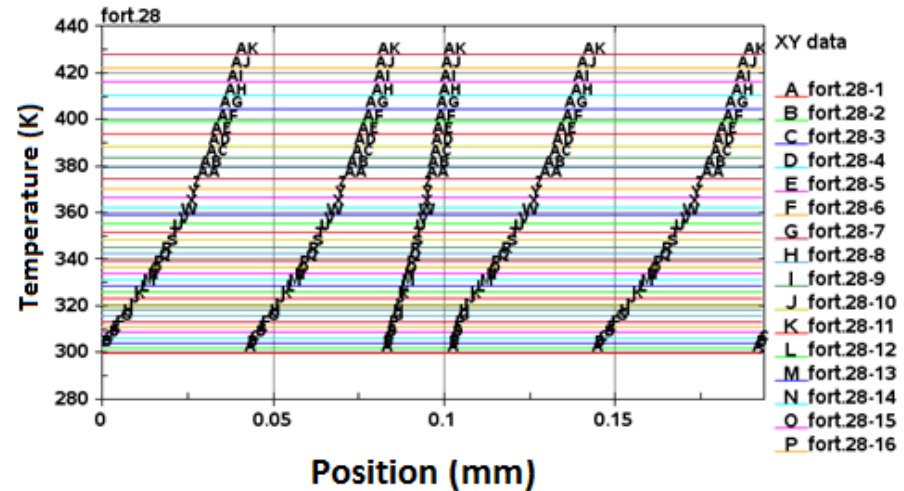
$$\begin{Bmatrix} \sigma_{=} \\ \sigma_{\perp} \end{Bmatrix} = \begin{bmatrix} C_{=} & C_{\times}^T \\ C_{\times} & C_{\perp} \end{bmatrix} \begin{Bmatrix} \epsilon_{=} \\ \epsilon_{\perp} \end{Bmatrix}$$

C. Zhang, J. Xu, L. Cao, Z. Wu, S. Santhanagopalan, 2017. *Journal of Power Sources*, 357, pp. 126-137.

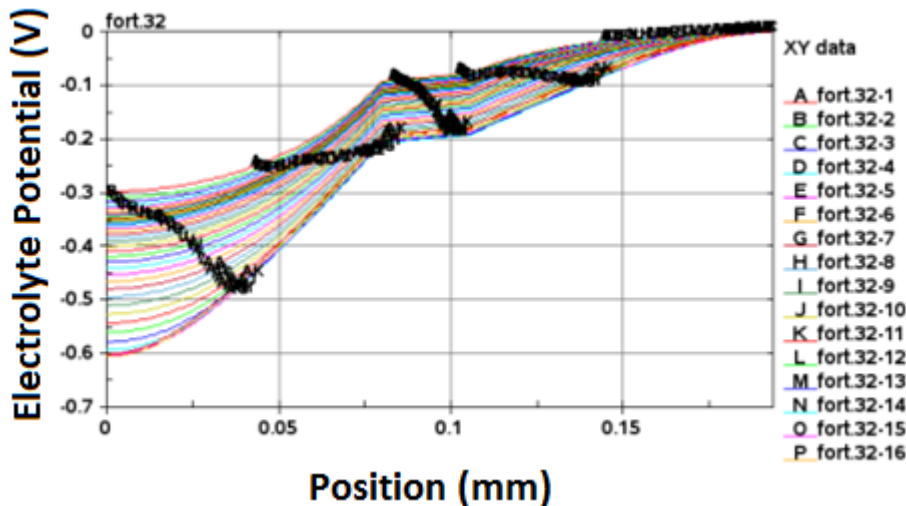
FY17 Accomplishments: Electrochemical Models in LS-DYNA

- First-ever case of implementing simultaneous simulation of ECT and mechanical models all in one place
- No need to switch back and forth between LS-DYNA and ANSYS (or other tools for ECT)
- Can use any custom ECT model (within reason)
- Can implement custom time-steps for each domain/physics (or keep it all the same)
- Can simulate a lot more physics (e.g., creep failure across several cycles, separator melting, etc.) than just mechanical crush simulations

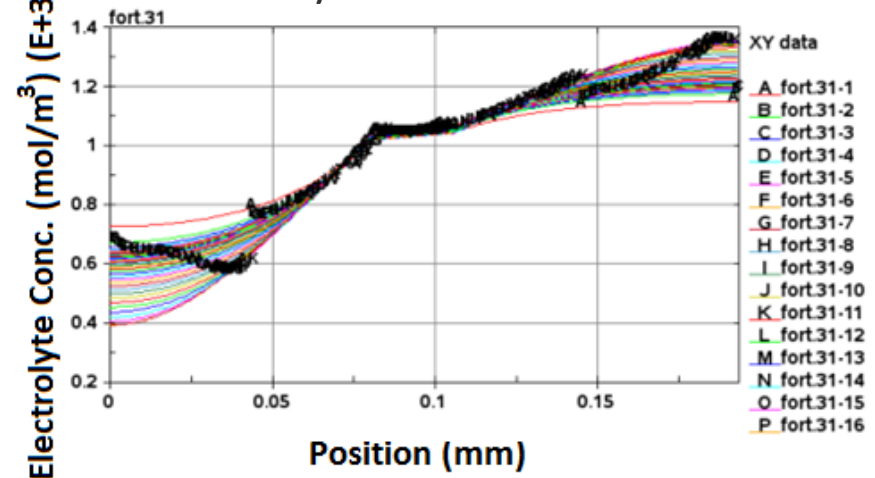
Internal Temperature



Electrolyte Potential

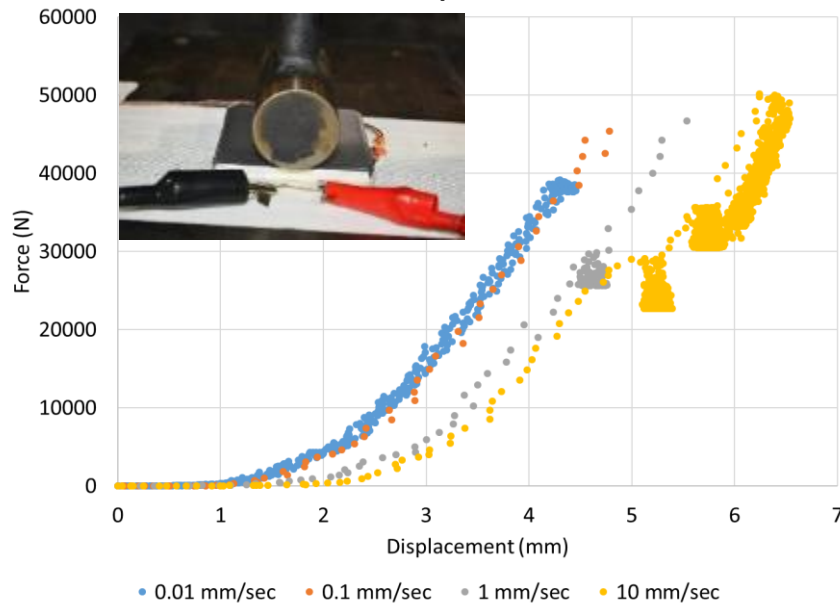


Electrolyte Concentrations



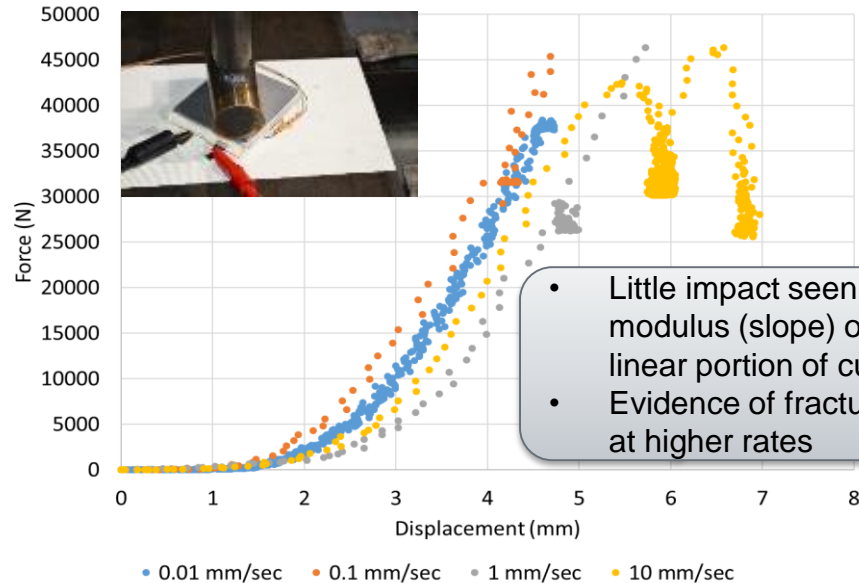
Strain rate studies – Cell Level Experiments at SNL

Orientation parallel to tabs



- Little change observed in overall modulus (slope) of these tests
- Lower force required to reach higher displacement in higher rate tests
- Signs of fracture failure at higher rates

Diagonal orientation



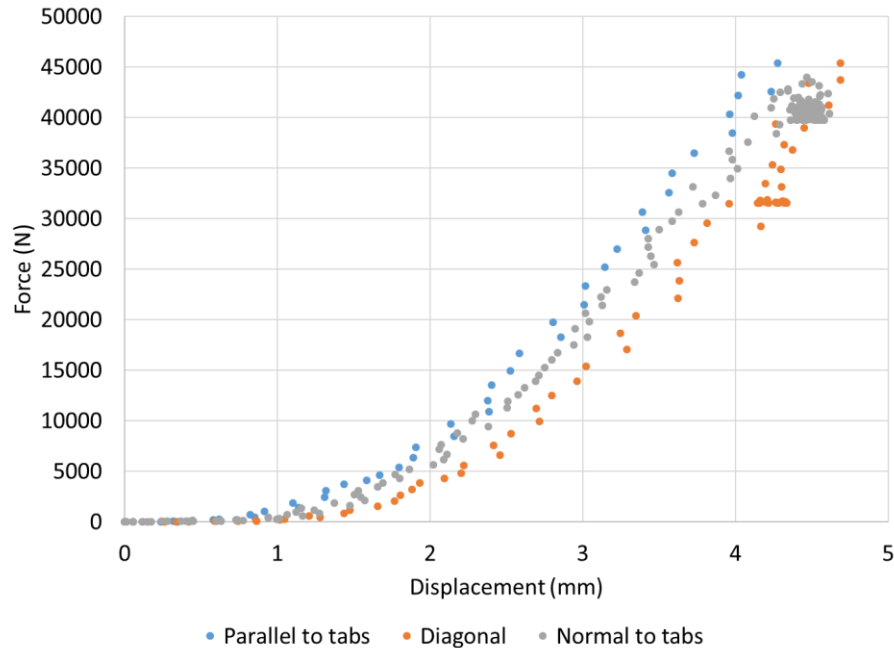
- Little impact seen in modulus (slope) of linear portion of curves
- Evidence of fracturing at higher rates

*Note: displacement was used as the end condition but control limitations at higher rates lead to some variations in end point
0 displacement for all tests corrected to the point where 10 N is first observed in the force measurement

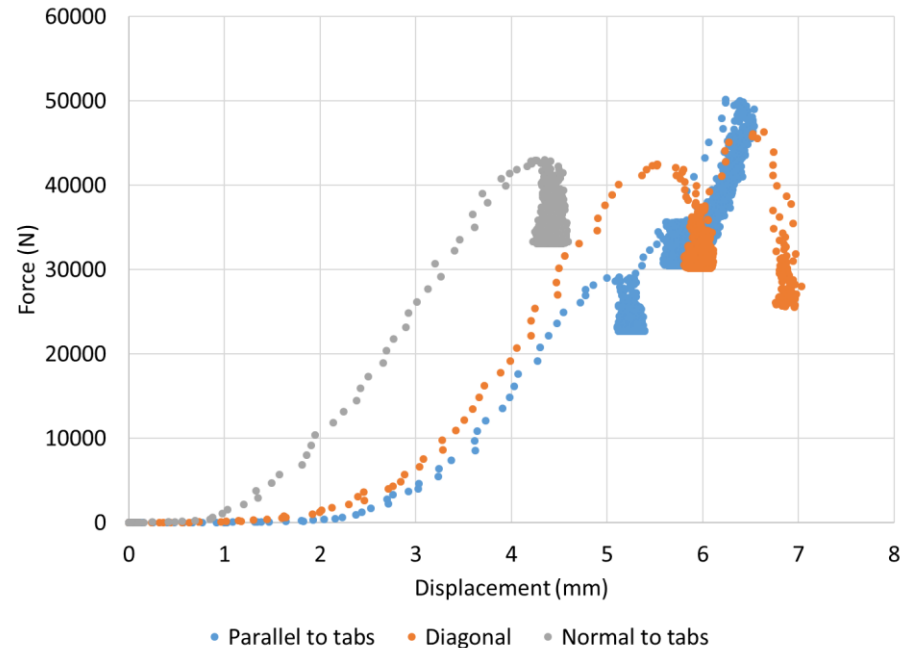
- Cell-level characterization at SNL covered the following aspects:
 - different orientations for the impact - strain rate (between 0.01 and 10 mm/sec)
 - ambient temperature
- Complex load conditions (e.g., 3-point bending) were added to the test matrix based on feedback from the reviewers last year
- Higher strain rates are being considered – Please See Future Work

FY17 Accomplishments: Comparison of orientations

0.1 mm/sec

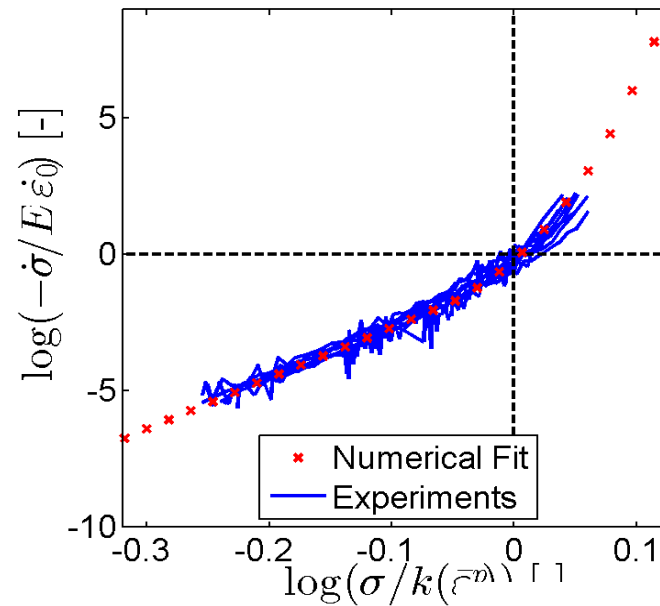
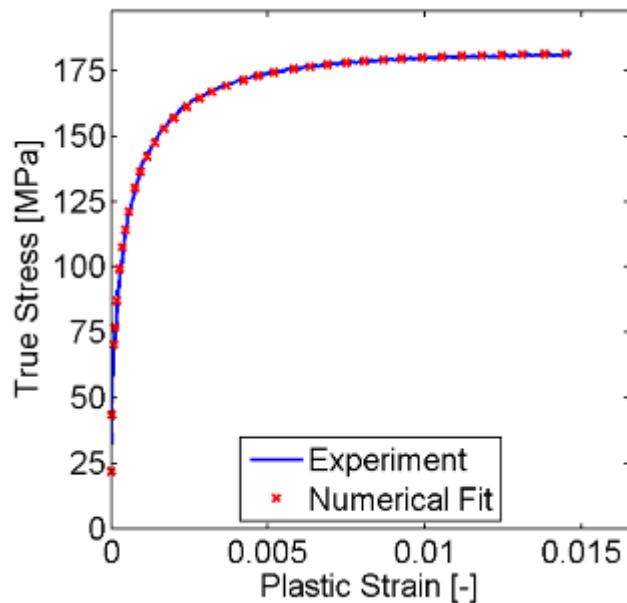


10 mm/sec



- Variation observed at higher rates – lower rates show little meaningful difference
- At higher rates some differences in both low rate data, some evidence of fracturing was observed in two of the three cases

FY17 Accomplishments: Constitutive Response during Failure Progression



Journal of Power Sources xxx (2017) xxx-xxx



Contents lists available at ScienceDirect

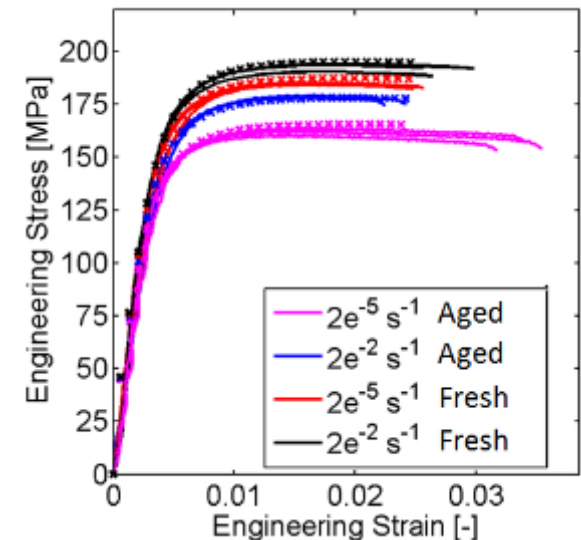
Journal of Power Sources

journal homepage: www.elsevier.com



Constitutive behavior and progressive mechanical failure of electrodes in lithium-ion batteries

Chao Zhang^{a, b}, Jun Xu^{c, d}, Lei Cao^a, Zenan Wu^a, Shriram Santhanagopalan^{a, *}



FY17 Accomplishments: Properties for Aged Cell Components

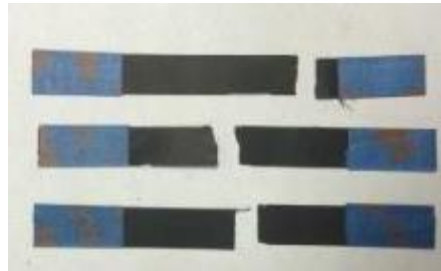


Fresh and aged 40-Ah PHEV cells (NMC-LMO/Gr) were cut open to characterize effect of aging

Compression Tests

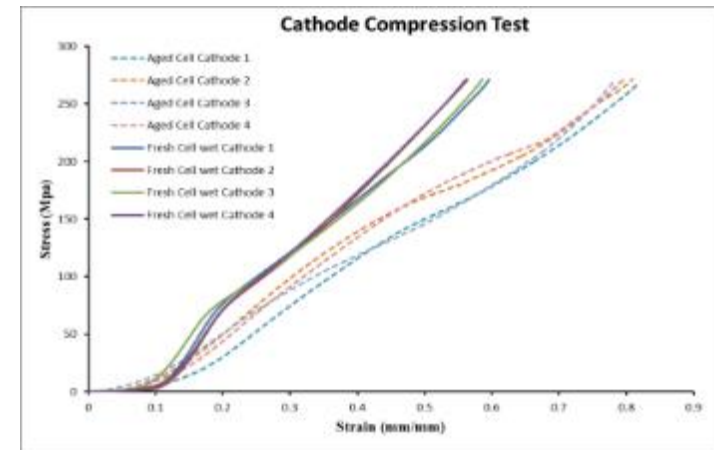
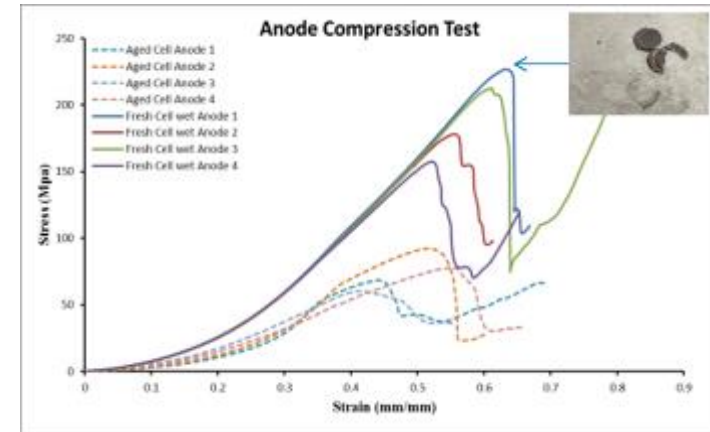
Before After

Tension Tests



S. Santhanagopalan, Presented at the International Battery Safety Workshop, June 2017, Albuquerque NM

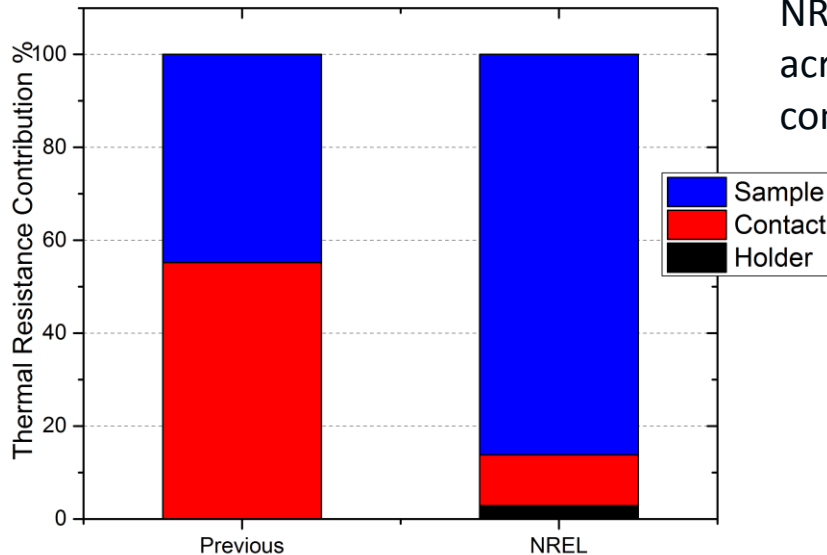
- Cells aged under six different conditions (temperatures, charge rates, discharge rates, voltage windows) were disassembled for characterization.
- Properties for the active material were regressed based on composite structure response
- Aged samples have lower ultimate strength and fail at lower strain values compared to fresh samples.
- Temperature has the highest effect on the mechanical properties, followed by charge rates. Voltage window had the least influence.



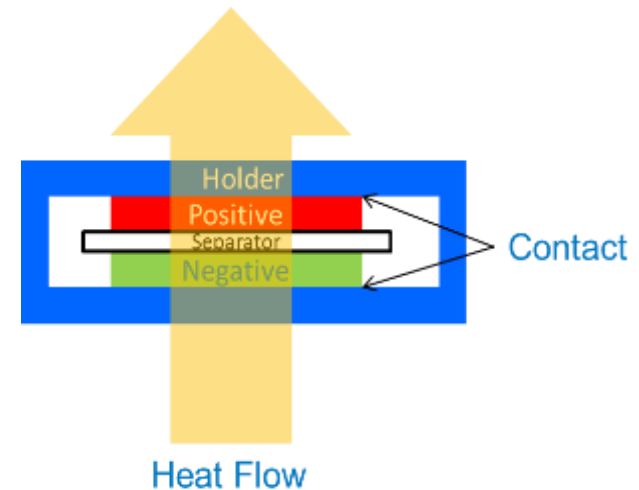
Constitutive response of fresh vs. aged cell components: Tensile test results show larger variability due to non-uniformity within the 4" x 1" sample, whereas the compression test results are uniform due to smaller sample sizes (1" dia. disc)

PHEV: plug-in hybrid electric vehicle

FY17 Accomplishments: Thermal Properties of Aged Cell Components

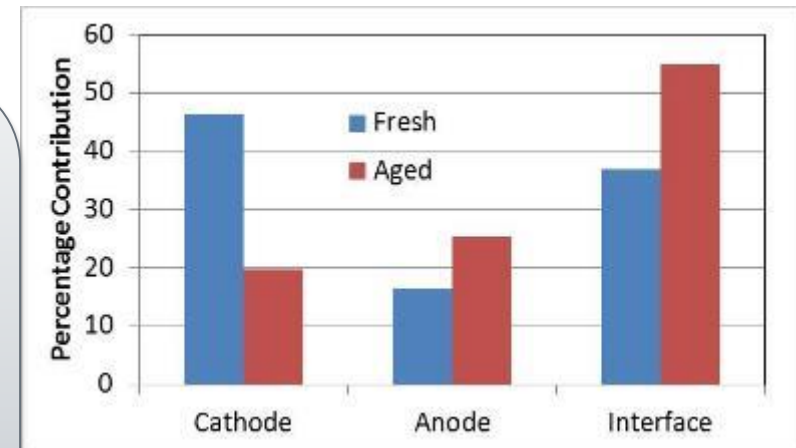


NREL's custom fixture to measure thermal impedance across cell components minimizes error due to poor contact between test articles and cell fixture.



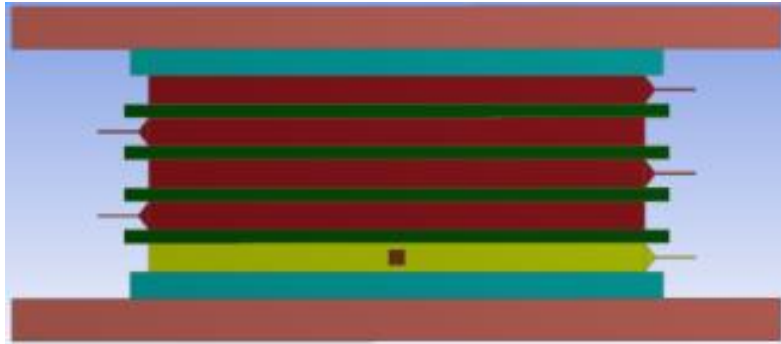
S. Santhanagopalan, Presented at the International Battery Seminar, March 2017.

- Contributions from sample holder in contact with the cell should be corrected for before changes due to electrode aging can be observed.
- Previous results in the literature were not sensitive to distinguish contact versus component thermal resistances.
- We designed a custom fixture to characterize thermal properties of wet and dry samples from fresh vs. aged cells.
- Interfacial impedance is an important but often neglected factor controlling heat generation rates in aged cells.



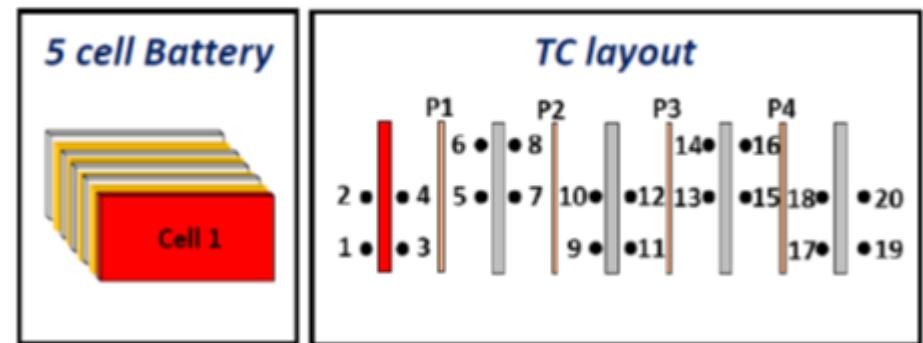
Interfacial thermal resistance increases significantly with aging

Failure Propagation: Multi-Cell Response (SNL)



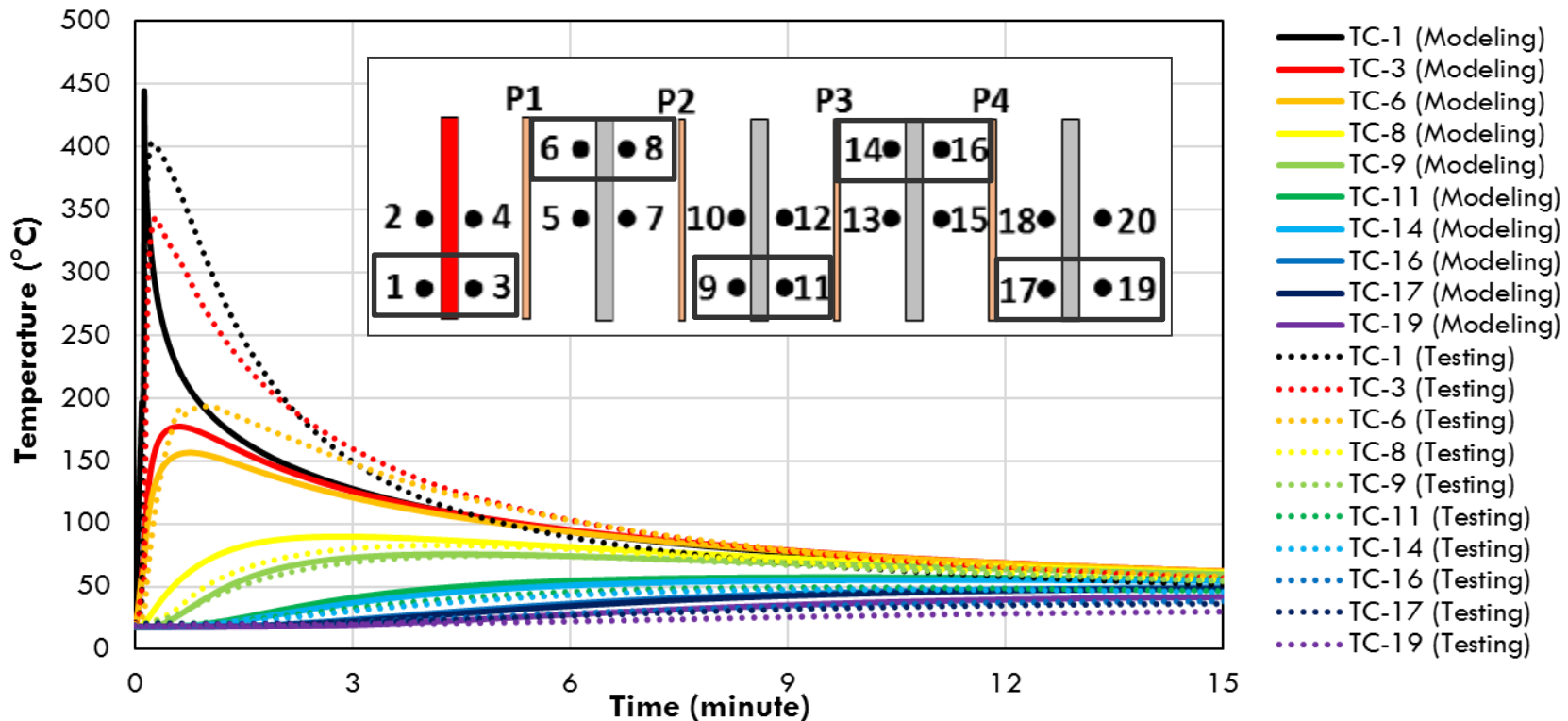
Excel ID	Test Description
Baseline	No thermal management
A-1	1/8 inches Al plates between cells
A-2	1/16 inches Al plates between cells
A-3	1/32 inches Al plates between cells
C-1	1/8 inches Cu plates between cells
C-2	1/16 inches Cu plates between cells
C-3	1/32 inches Cu plates between cells

Copper or Aluminum Plates (P1,P2,P3,P4)



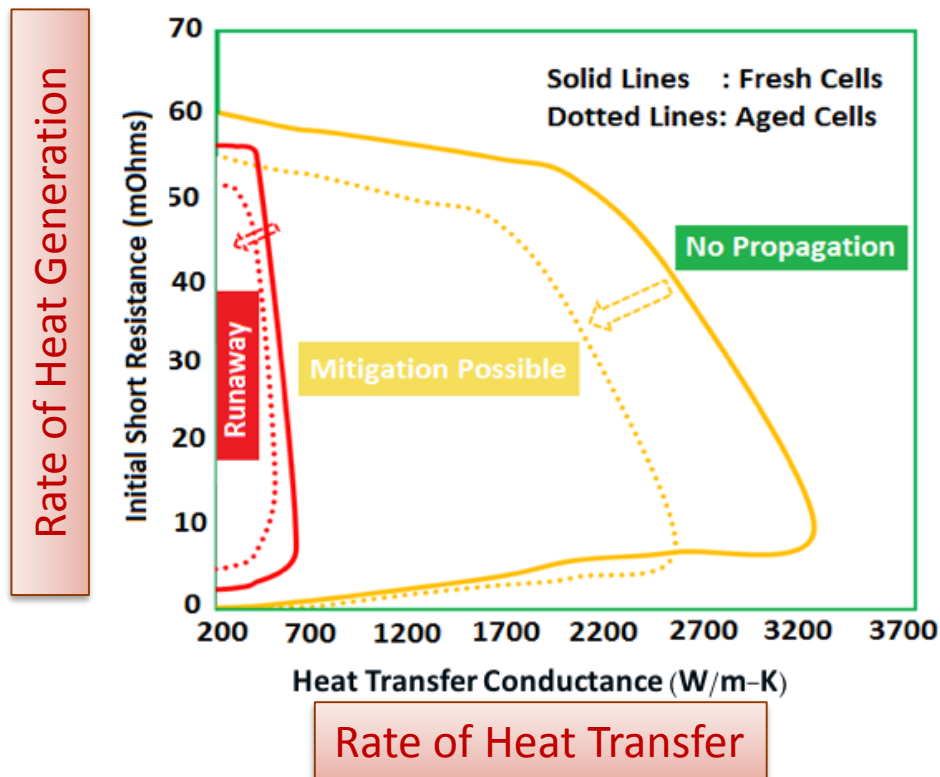
- 3-Ah COTS LiCoO₂ pouch cells were assembled into modules of 5 cells at SNL and packaged against different heat sinks (A1-C3).
- One cell was subjected to failure by mechanical nail penetration, and propagation was monitored using thermocouples shown along locations 1-20.

Failure Propagation: Validation of Multi-Cell Simulations

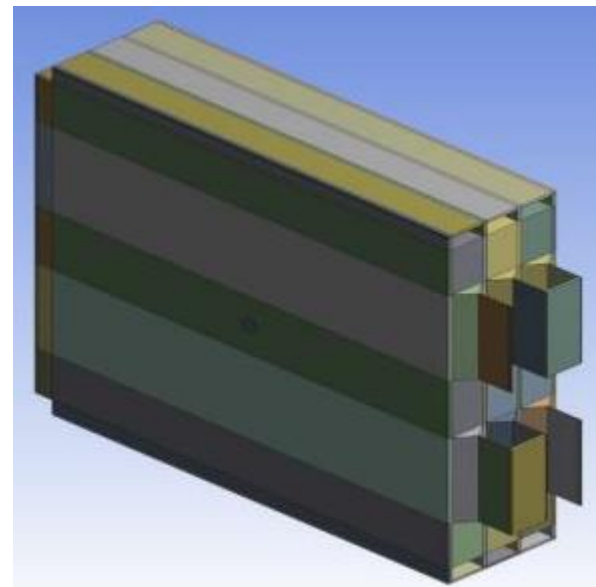


- Overall, the simulation results show a fairly good agreement with the test results.
- The top three reasons for differences between predictions and data were:
 - Assumption made in the lumped thermal model about instantaneous heat release at the trigger cell (whereas in the experiments, heat release was spread out across 5.5 sec)
 - Contact between the cells and cooling plates, as well as that between the thermocouples and the cells are not well controlled in the experiments
 - Factors such as release of smoke and heat from the ejecta are not captured by the model

FY17 Accomplishments: Failure Propagation in Aged Modules



- 3S1P module
- 24-Ah LCO/graphite
- Shutdown separator
- Fin cooling
- Initial internal short circuit in the middle cell



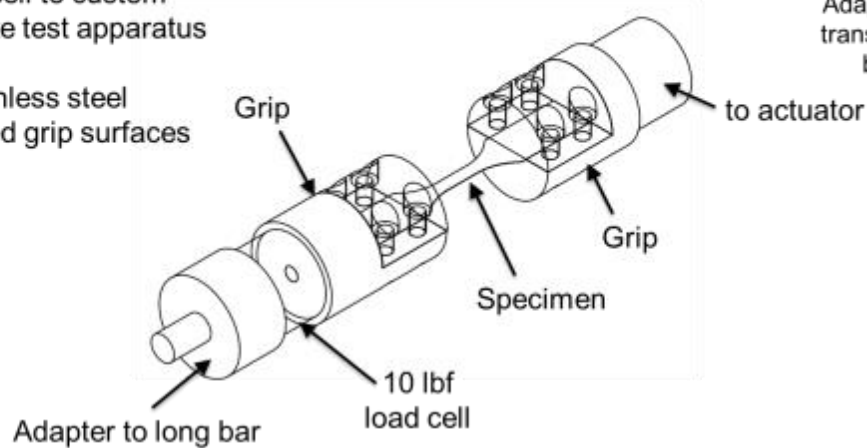
- Based on the results from previous slides, we built a generic “safety map” that plots heat generation rate versus heat dissipation rate for different failure modes.
- This plot is independent of the type of cells or test conditions: the runaway (red) and mitigation (yellow) zones are defined by the end user based on constraints imposed by the design of the module (e.g., max. possible form factor or cooling-plate thickness, etc.)
- For majority of failure scenarios, we observed that the cells get safer with aging due to lower energy content, but we did not account for an increased probability of failure in aged cells.

Future Work....

- Dynamic loading tests are required to characterize failure at higher strain rates.
- The OSU team is exploring test fixtures that will build the data set to populate constitutive relationships under these conditions.

Dynamic tension fixture Design

- Fixtures designed to adapt 10lbf load cell to custom intermediate test apparatus (long bar)
- 7/8 in. Stainless steel
- Sandblasted grip surfaces

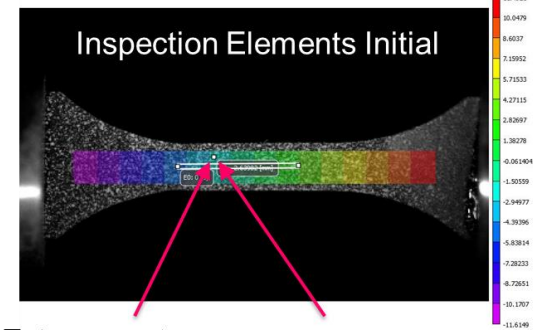
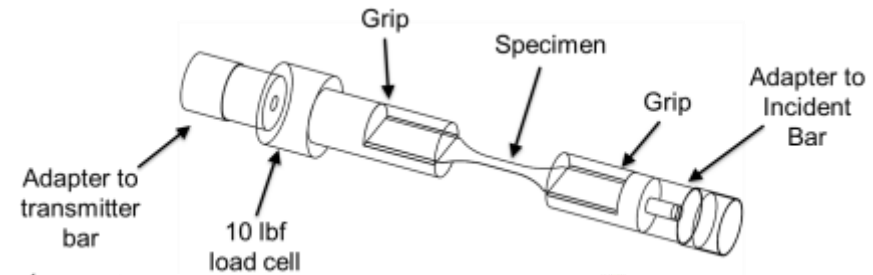


- Strain rates of 1,000-5,000/s
- Torsion/shear tests across different orientations
- Temperature controlled

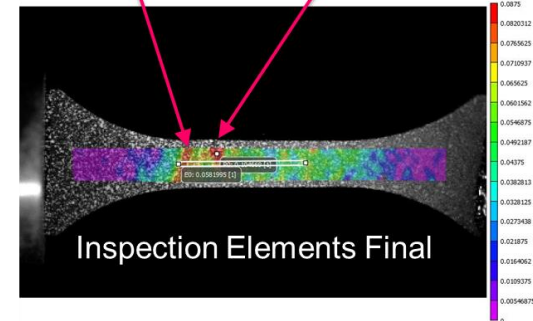
Processing digital image correlation data on multi-axial deformation

Figure Credits: Jeremy Seidt, OSU

Vice Design



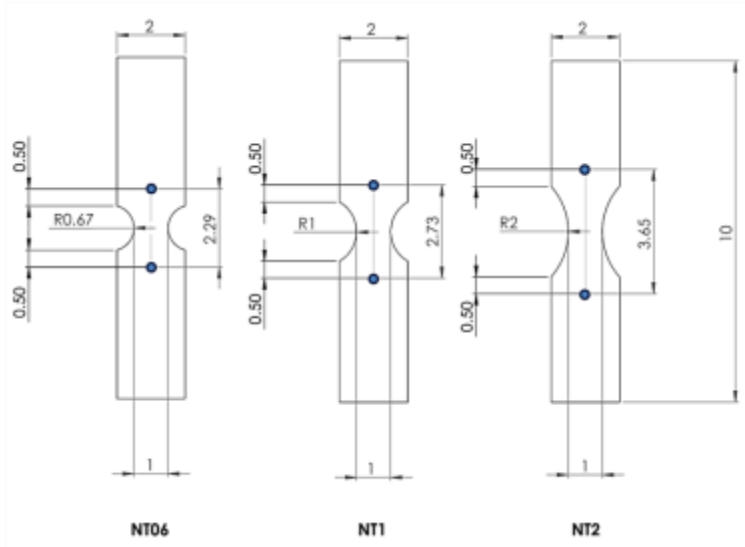
Extensometer



***Any proposed future work is subject to change based on funding levels.**

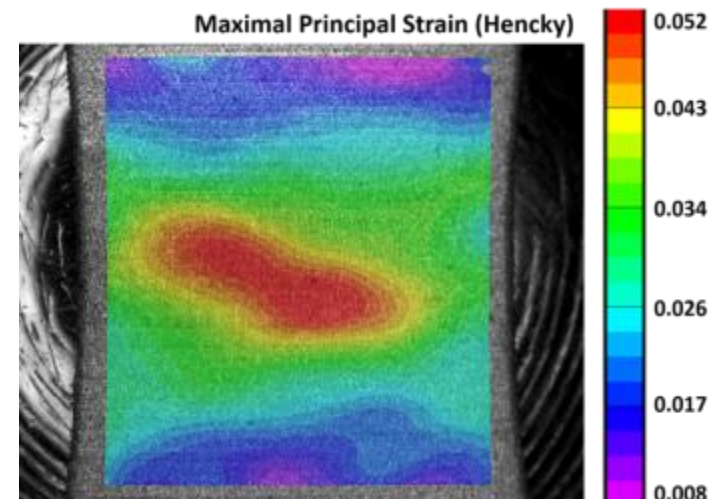
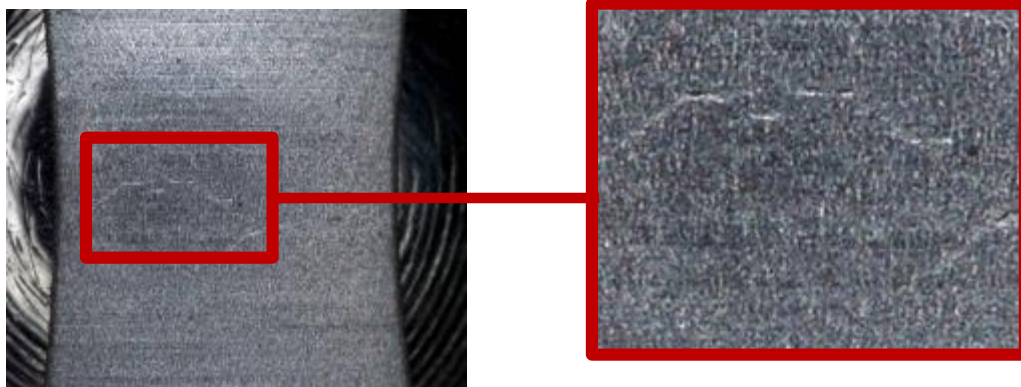
Future Work: fracture Experiments for Different Stress States

Notched tension experiments



- ❖ Fracture of different components on an electrode composite is a complex problem to simulate.
- ❖ The sample specifications, along with some sample results from the fracture experiments, are shown alongside.
- ❖ Digital image correlation was used to quantify observations.

Hasek Punch Tests – Digital Image Correlation



Response to Previous Year Reviewers' Comments

- Comment: How much of the material R&D data can be transferred to the computer-aided engineering of batteries (CAEBAT) tools? Is it necessary to develop a user material model to capture the material behavior effectively?
Response: In response to this reviewer's comment, we implemented a user-defined material model, along with user-defined elements that can have arbitrary degrees of freedom in LS-DYNA.
These tools now enable the end user to import materials data in the form of a csv file (to build a curve/look-up table within LS-DYNA) or to calibrate custom constitutive models (Zhang et al., *Journal of Power Sources*, 2017).
- Comment: Perhaps the future parameter identification research could consider temperature dependence.
Response: We have included temperature as a factor in SNL's cell tests for validation. The NREL/OSU team already has similar data at the component level. Aging effects on thermal impedance have been included this year.
- Comment: One of the reviewers suggested that we include a design of experiments (DOE) fractional or full factorial study with reduced set of experiments considering sample input and output.
Response: We have included a table listing the test matrix on Slide 10.

Response to Previous Year Reviewers' Comments (Contd.)

- Comment: In terms of future work, the project is using an explicit FEA model (LS-Dyna) but the strain rates that the project are experimentally testing at are static. The reviewer recommended quickly moving on to higher strain rates, this is what LS-Dyna was made to look at.
Response: In response to this reviewer's comment, we are currently evaluating experimental results at high strain rates (1,000-5,000/s) using a dynamic tension fixture working together with the OSU team.
- Comment: The reviewer was not sure why the project is using LS-Dyna when it could get DOE version Dyna3d or Paradyn. The reviewer said that another good software that could model the liquid electrolyte would be CTH out of SNL and that maybe collaborating with someone at Lawrence Livermore National Laboratory would provide you with the source to Dyna and more development possibility.
Response: At the beginning of this project, the team was new to LS-Dyna; a poll of end users identified LS-DYNA as the choice for explicit simulations; support from LSTC has been helpful throughout the last few years, in addition to the models being readily accessible to the end-users.
We will consider use of Dyna3d as part of our on-going efforts. We are teaming up with the SNL team on a parallel effort to model electrolyte failure.

Collaborators and Partners

Industry Advisory USCAR/CSWG

Bill Stanko, Yibing Shi,
Saeed Barbat,
Guy Nusholz

Project Leader
NREL, Kandler Smith

Task 1 PI
Shriram
Santhanagopalan

Task 2 PI
Shriram
Santhanagopalan

Task 3 PI
Kandler Smith

**Cell/Electrode
Making**
ANL, Daniel Abraham,
Pierre Yao, Dennis
Dees

**Material
Characterization**
OSU, Amos Gilat

Abuse Testing
SNL, Joshua Lamb

Integration with ANSYS and LS-DYNA,
FST, Kelly Carnie; GMU, Paul Dubois

Microstructure Modeling
Purdue, Partha Mukherjee

Fabrication/Testing
ANL, Daniel Abraham,
Pierre Yao

Key Contributors:

- Leigh Anna Steele, SNL
- Chris Grosso, SNL
- Jerry Quintana, SNL
- Loraine Torres-Castro, SNL
- June Stanley, SNL
- Andrew Jansen, ANL
- Genong Li, ANSYS
- Chuanbo Yang, NREL
- Qibo Li, NREL

Summary

- **Task 1**. A Newman model was calibrated to show agreement of a macro-homogeneous model against the entire CAMP library.
 - Publication: F.L.E. Usseglio-Viretta, et al., *J. Electrochem. Soc.*, under review.
- **Task 2**. Simultaneously coupled mechanical-electrochemical-thermal model for mechanical abuse simulation
 - A user-defined material model was developed that enables the users to import experimental data for mechanical characterization of cell components to define constitutive relationships.
 - Effect of aging on mechanical, thermal (as well as electrochemical) response of the cells and cell components was characterized experimentally and validated against model predictions.
 - Propagation of failure from individual cells to multi-cell test articles is currently being investigated.
 - High strain-rate tests for cell components to simulate dynamic response of the cells are underway.

See Complete list of publications in the last section of this presentation.

Acknowledgements

- We appreciate support and funding provided by Vehicle Technologies Office at the U.S. Department of Energy
 - Brian Cunningham
 - Samuel Gillard
 - David Howell

Technical Back-Up Slides

Mechanism of Failure Initiation Following a Crush

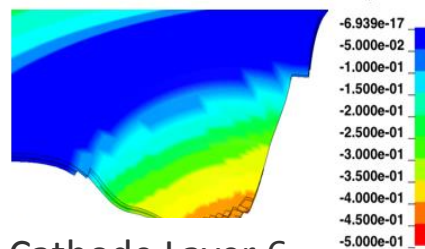
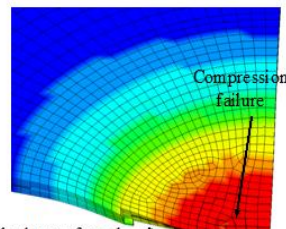
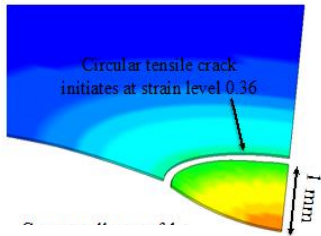
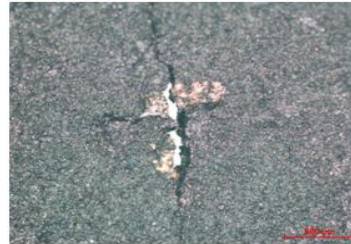
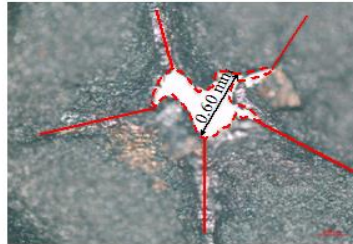
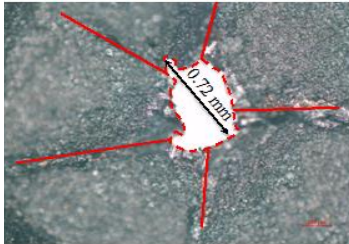
1st layer

4th layer

7th layer

Sahraei et al. *Journal of Power Sources*, 2014

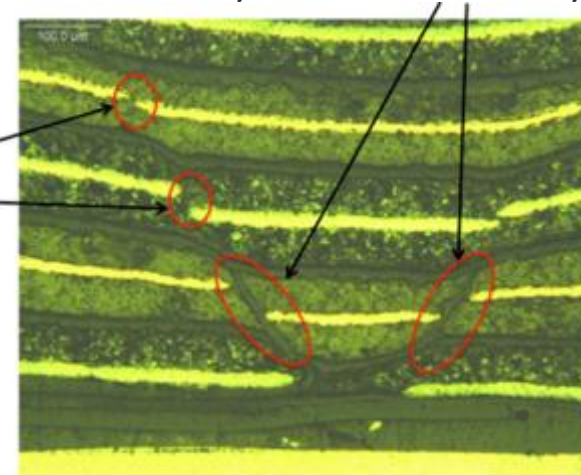
Side facing
the indenter



Cell-level crush tests used
to have a “pass” or “fail”



Shear failure of active material
layers within a battery



Copper foil
fails before
separator
ruptures

Wang, Shin et al., *Journal of Power Sources* 306 (2016): 424-430.

Outcome

- Comprehensive understanding of failure thresholds and propagation mechanism for each component within the cell
- Better explanation of test data results and recommendations for test methods
- Light-weighting/right-sizing of cells without compromising safety

Copper foil Layer 1
Failure of Copper Foil

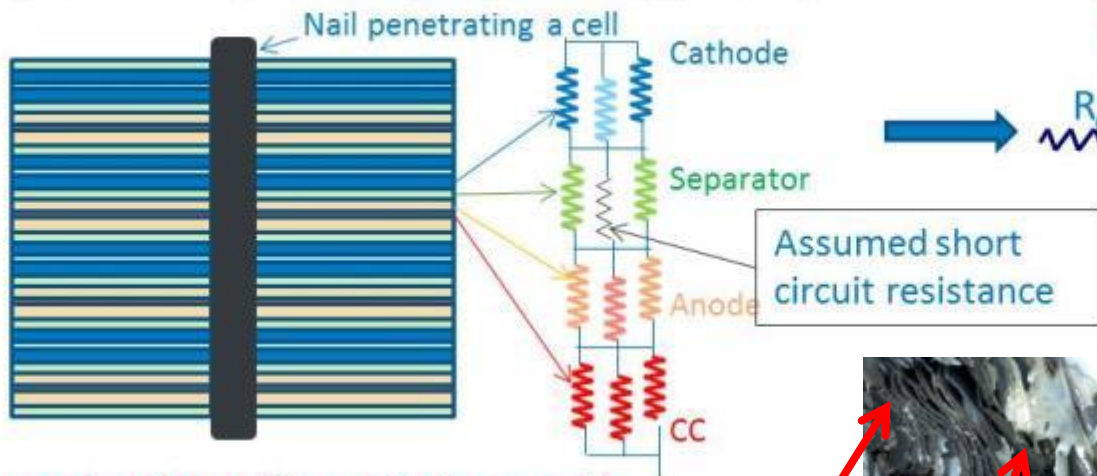
Anode Layer 4

Cathode Layer 6
Cathode-Anode Short

C. Zhang et al., *J. Power Sources*, Accepted (Mar. 2017)

Estimating Short-Circuit Resistance

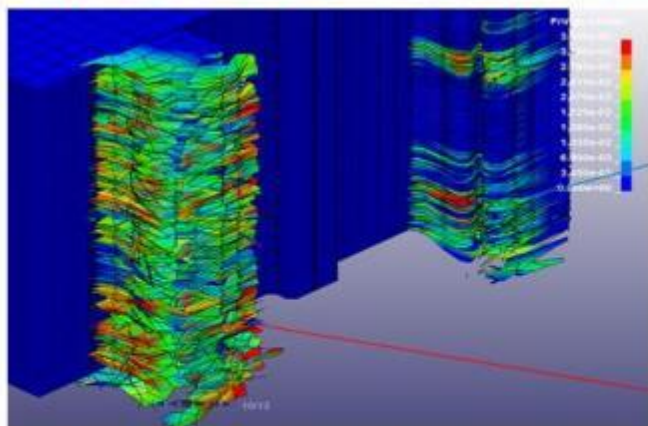
Regular Short (Previously Reported Approach):



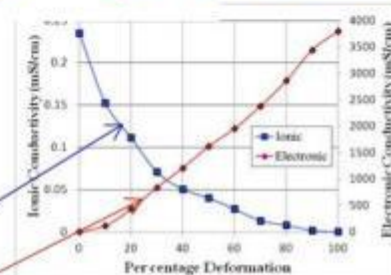
Gi-Heon Kim, 6th Lithium Mobile Power Conference, Boston MA, 2010.

Kalupson et al., ECS Spring Meeting, Orlando FL, April 2014.

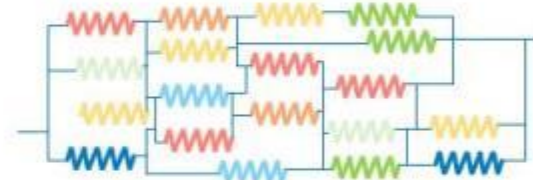
Irregular Short (Current Approach):



Deformed geometry obtained using CAD geometry of cells subjected to crush in LS-DYNA simulations



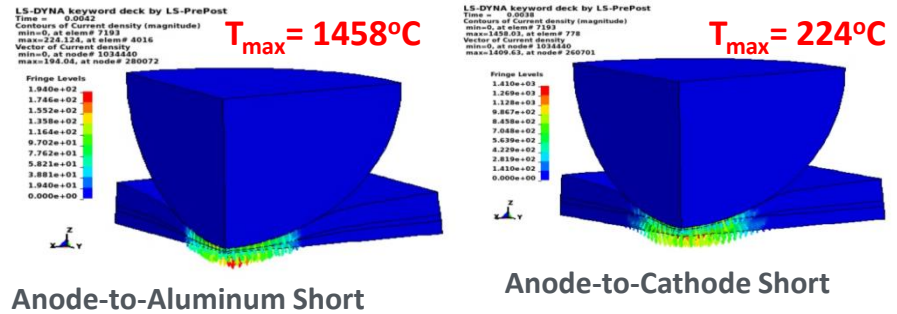
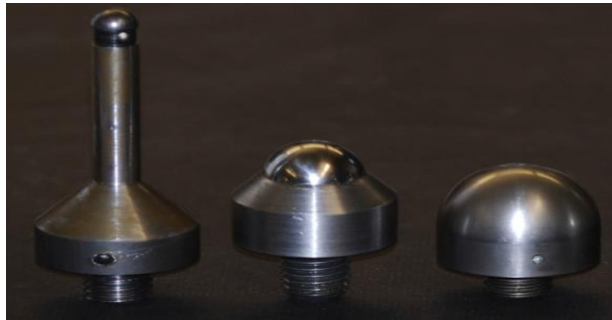
Use ionic and electronic resistivity of the deformed layers change as a function of thickness



Calculate short resistance by solving Maxwell's equations in Ansys or DYNA using deformed geometry and properties of individual layers

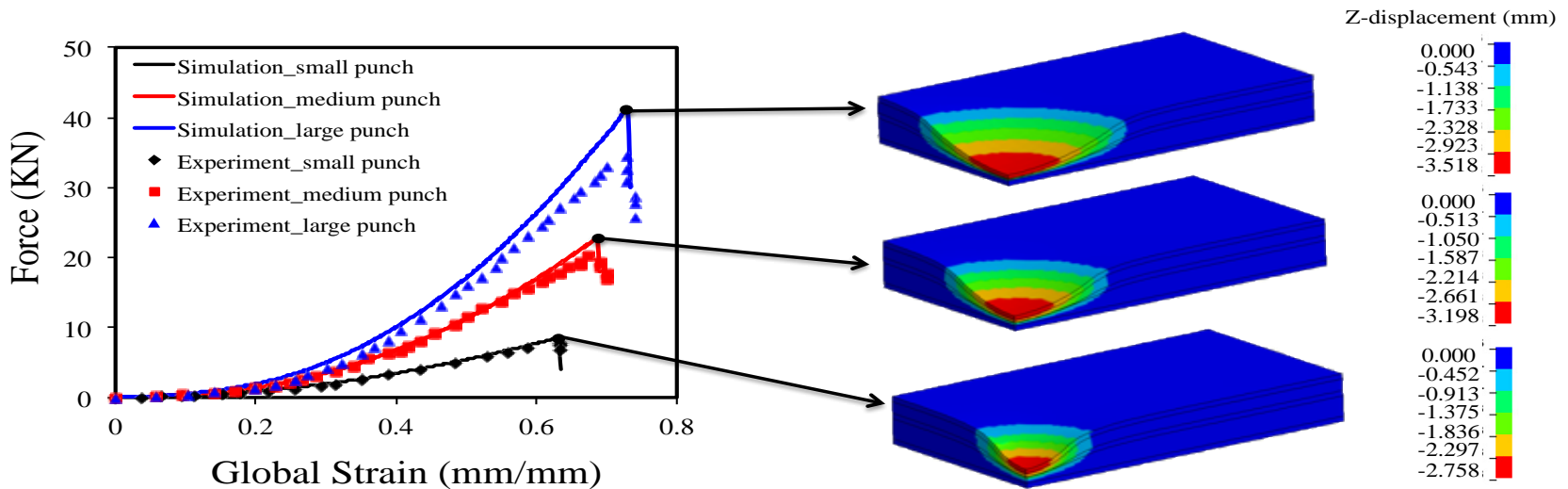
Cell-Level Results

Sahraei et al., *Journal of Power Sources*, 2014



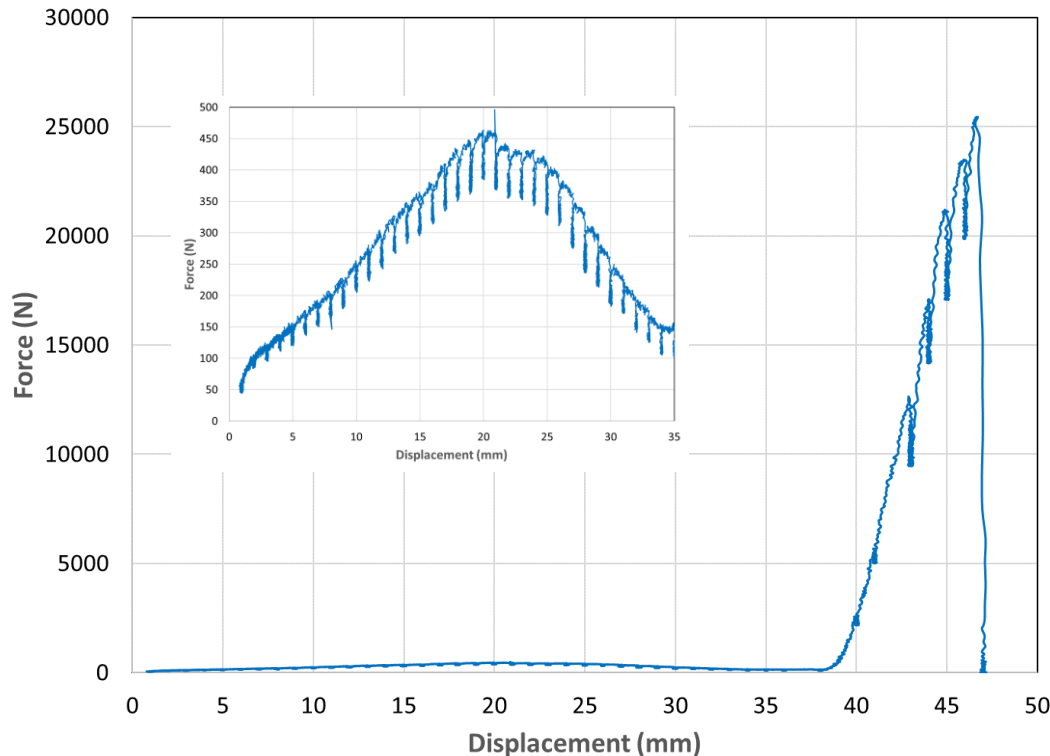
Cell Thermal Response under various types of short-circuit

S. Santhanagopalan, Presented at the International Battery Seminar & Exhibit, 2017.



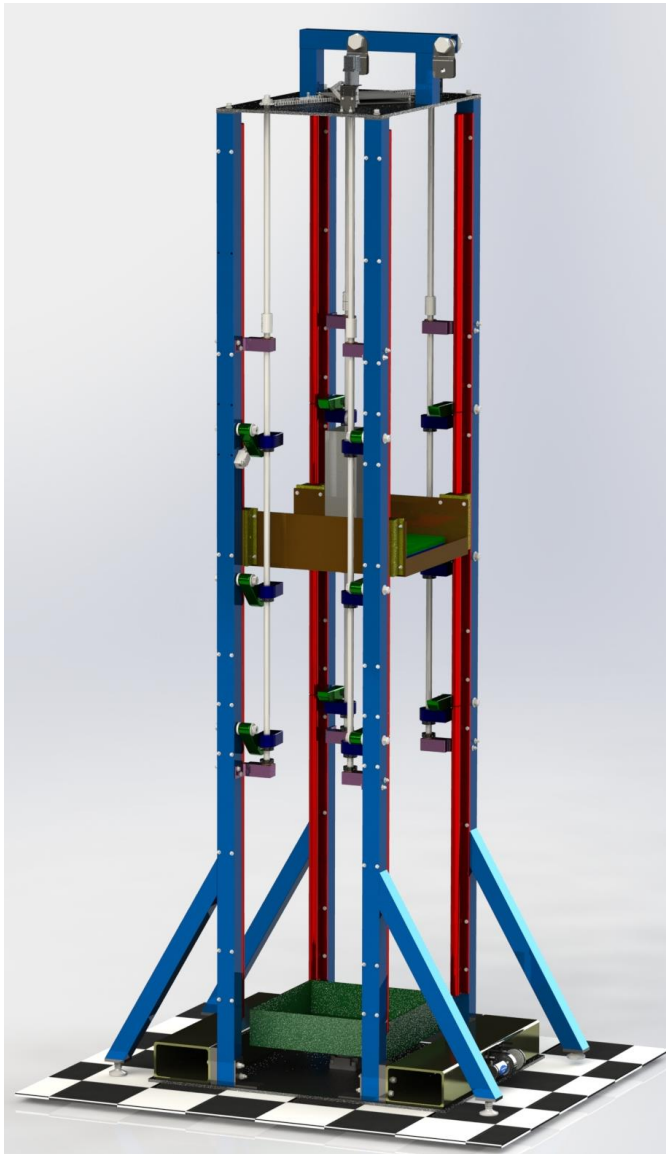
Models adequately capture mechanical and thermal response under different test conditions.

Three-Point Bend Test – Fully Charged Cell



- Bend portion of test shows a yield of ~ 450 N.
- Cell failure required a compressive force of ~ 25 kN.
- “Pre-load” portion of bend observed where initial compression is applied to cell before bending occurs.
- After yield of cells to bend the cell is put into compression.

Drop Tower – Impact Tester



Specifications:

- Overall height: 14 feet (4.3 m)
- Drop height: up to 10 feet (3.1 m)
- Drop weight: 50 to 500+ pounds (22.7 – 226.8 kg)
- Max impact velocity ~ 25.4 ft/s (7.74 m/s)
- Impact force (assuming a 6" stopping distance): 10,000 lbs-f (44,482 N)
- Remote operation
- Data collection:
 - Displacement
 - Impactor velocity
 - Force at impact
 - Temperature
 - Voltage

Figure Credit: Joshua Lamb, SNL

Drop Tower – Impact Tester

Current Status:

- ✓ CAD model – complete
- ✓ Drawing package – complete
- ✓ Hardware bill of materials (BOM) – complete
- ✓ Controls box design – complete
- ✓ Controls BOM – complete
- ✓ BATLab personnel to order all controls hardware – near complete
- ✓ Build complete
- ✓ Commissioning and initial experimentation underway

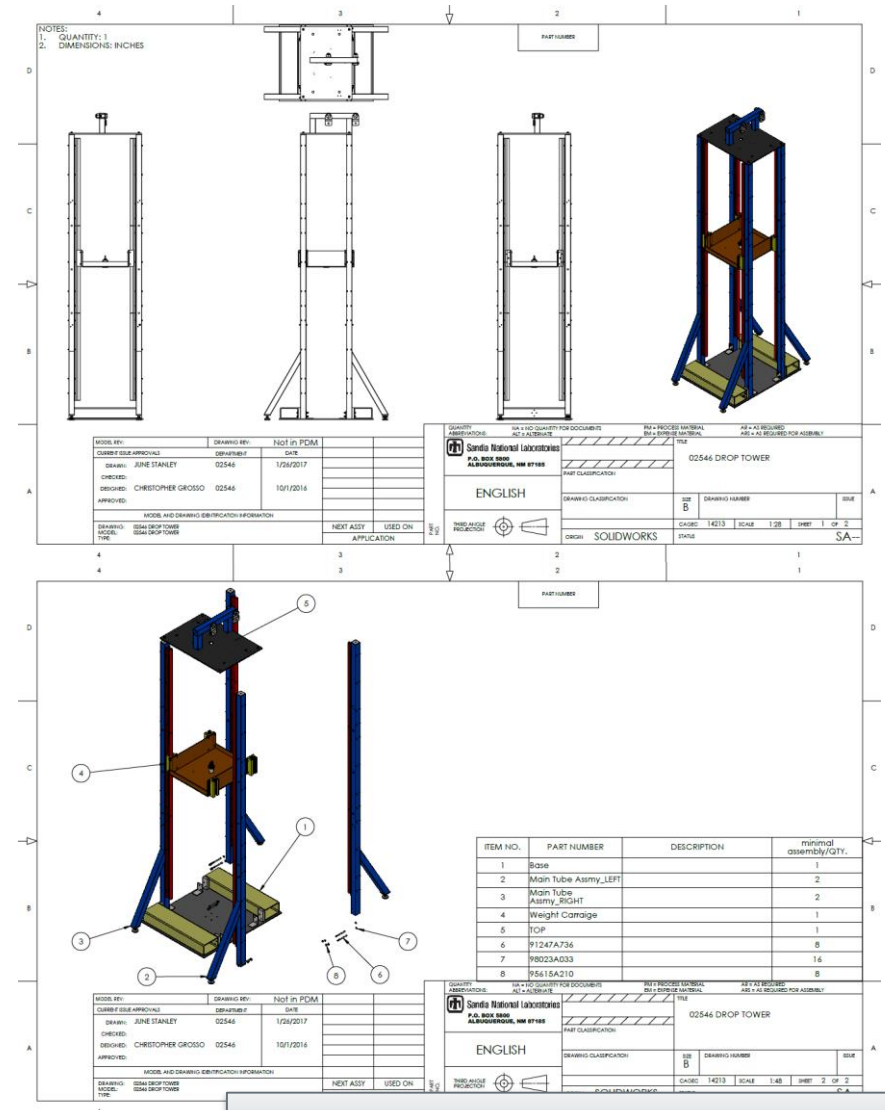


Figure Credit: Joshua Lamb, SNL